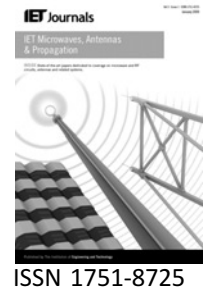


Published in IET Microwaves, Antennas & Propagation  
 Released for publication on 28th April 2008  
 Received on 29th January 2008  
 Revised on 28th April 2008  
 doi: 10.1049/iet-map:20080033



# Diagnostic of phased arrays with faulty elements using the mutual coupling method

Y. Neidman<sup>1</sup> R. Shavit<sup>1</sup> A. Bronshtein<sup>2</sup>

<sup>1</sup>Department of Electrical and Computer Engineering, Ben-Gurion University of the Negev, Beer Sheva 84105, Israel

<sup>2</sup>Elta, Ashdod 77102, Israel

E-mail: rshavit@ee.bgu.ac.il

**Abstract:** The ability to calibrate phased array antennas by utilising the mutual coupling method (MCM), which takes advantage of the mutual coupling effect between adjacent elements, is addressed. The basic assumption of the method is that the mutual coupling between adjacent elements is equal for all elements in the array and its major deficiency is its failure in the case of faulty elements. A parametric study to identify the effect of faulty elements in the array has been conducted. It has been shown that displacement of one element in the array may cause a significant error in the calibration, which affects its radiation characteristics (increase in the far side lobe level). The main contribution is the presentation of the effect of faulty elements in the calibration process and the proposal of a way to detect and bypass the faulty elements in a phased array calibrated by the MCM.

## 1 Introduction

Active phased array antennas work at their peak performance when they are well calibrated. Moreover, to maintain full operability in both the transmit and receive modes, it is important that the phased array elements should be calibrated for the amplitude and phase in both modes. Initial calibration of the antenna elements is done at the factory and sustained high operability and performance necessitates additional calibration from time to time.

There are some known calibration methods such as: calibration using an embedded special designed network, calibration using external antennas and calibration using special purposed internal antenna elements. These methods are described in [1, 2]. In all these methods a calibration table is generated in an indoor near field range which is used for reference in the on site calibration procedure. This calibration table should be renewed every few years in the indoor near field range. Phased array antennas, which are used for ground-based radars, are extremely large and difficult for transportation, and require huge near field range facilities for the testing/calibration procedures. Therefore calibration of these antennas on site without the necessity of an indoor near field range is important. Calibration using the mutual coupling method (MCM) addresses this necessity and enables a cost effective calibration on site.

The MCM was first introduced by Aumann *et al.* in [3] for phased arrays with monopole elements and used by Shipley and Woods in [4] with dipole elements. The method uses the mutual coupling between adjacent elements for calibrating the amplitude and phase of the elements in the array. Using the MCM, the antenna manufacturers are released from the need to use near field range calibration techniques for an on site antenna (outdoor) calibration. The MCM procedure can be implemented only on antennas that are designed with three basic requirements: separate or well isolated transmit and receive ports, individual control of attenuation, phase and on-off switching for every element and symmetrical radiation patterns on the transmit and receive modes for every element. Its major deficiency is that faulty elements introduce calibration errors which propagate along the array. In this paper, a method of detecting faulty elements and bypassing them such that they would not affect the calibration of other elements is presented.

## 2 MCM calibration method description

The MCM is based on the assumption that the array elements can operate in both transmit and receive modes and for simplicity it will be explained only for a linear array. The method is based on the assumption that the

active reflection coefficient,  $S_{nn}^a(u)$  of the elements in the phased array is identical, which holds only in an infinite array. Moreover, this assumption can be made if the elements are equispaced and have symmetrical radiation patterns with respect to the normal of the array axis. In a finite length array with  $(2N_x + 1)$  elements and inter element spacing  $d$ , the active reflection coefficient of the  $n$ th element can be computed by

$$S_{nn}^a(u) = \sum_{m=-N_x}^{N_x} S_{mn} \exp\left[-jmd \frac{2\pi}{\lambda} \sin \theta_0\right] \quad (1)$$

in which the mutual coupling scattering parameters  $S_{mn}$ ,  $m, n = -N_x, \dots, N_x$  are summed on all excited elements in the array with the proper phase to obtain the peak beam in the direction  $\theta_0$ . The parameters  $S_{mn}$  can be computed or measured for each excited element in the array with all other elements terminated. However, only the close-in elements to the  $n$ th element have a major effect, since the mutual coupling decreases with distance. Consequently, the active reflection coefficient of the edge elements is significantly different from that of the centre elements. This variation introduces considerable pointing errors of the resulting sum beam, especially in wide scan angles. This finding was systematically investigated in [5] and the solution suggested was to extend the array with dummy elements at the edges. Study of the behaviour of active reflection coefficients near the array edges can determine the required number of dummy elements. Fig. 1 shows the normalised active reflection coefficient for a typical linear phased array with 80 elements. The elements are  $\lambda/2$  long parallel dipoles in front of a conductive plane at a distance  $\lambda/4$ . One can observe that for a  $0^\circ$  scan the variation in the active reflection coefficient reduces to almost zero after two elements from the edge, whereas for a  $45^\circ$  scan the variation reduces to zero after five elements from the edge. In the MCM calibration procedure, the array elements are calibrated

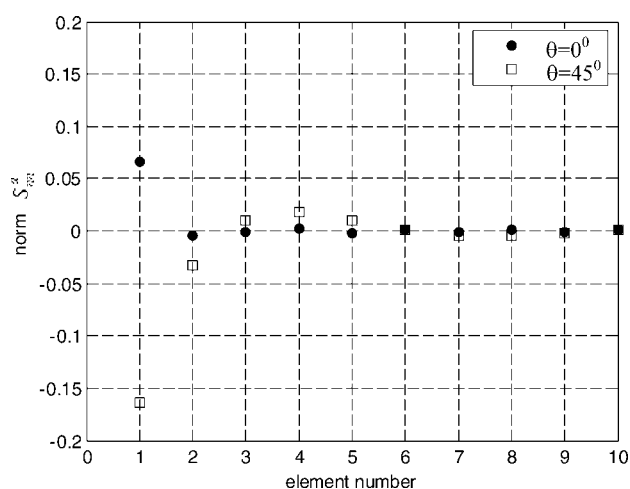


**Figure 1** Normalised active reflection coefficient in an 80-element linear phased array as a function of the element position relative to the array edge for  $0^\circ$  and  $45^\circ$  scans

for a  $0^\circ$  scan; therefore the addition of only two elements at the edges is sufficient to satisfy the requirement of identical active reflection coefficient for all elements in the array.

For the calibration purposes, the array is divided into two groups – even (ne) and odd (no) elements. The even elements use the odd elements for calibration, and vice versa. The connection between the two groups can be done using external equipment or utilising the method suggested by Shipley and Woods [4].

## 2.1 Transmit calibration

The calibration procedure in the transmit mode for the even elements is shown in Fig. 2 and outlined below:

1. Transmit with element (ne-2) and receive with element (no-1).
2. Transmit with element (ne-1) and receive with element (no-1).
3. Change the transmit parameters (amplitude and phase) of element (ne-1) such that the received signal with element (no-1) will be equal to that received when element (ne-2) is transmitting. At this point, elements (ne-2) and (ne-1) are calibrated relative to each other in the transmit mode.
4. Now, we can proceed with calibration of (ne) relative to (ne-1) using (no) and so on for all the even elements in the transmit mode.

In a similar manner, it is possible to calibrate the odd elements in the transmit mode using the even ones.

## 2.2 Receive calibration

The calibration procedure in the receive mode for the even elements is shown in Fig. 3 and outlined below:

1. Transmit with element (no-1) and receive with element (ne-2).
2. Transmit with element (no-1) and receive with element (ne-1).
3. Change the receive parameters (amplitude and phase) of element (ne-1) such that the received signal with element (ne-1) will be equal to that received by element (ne-2). At this point, elements (ne-2) and (ne-1) are calibrated relative to each other in the receive mode.

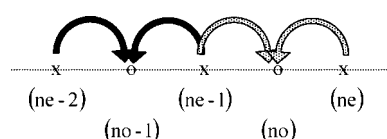


**Figure 2** Calibration of the even elements in the transmit mode

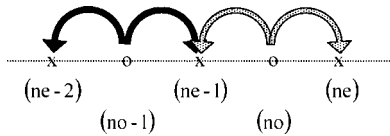


**Figure 3** Calibration of the even elements in the receive mode

4. Now we can proceed with the calibration of (ne) relative to (ne-1) using (no) as a transmitter and so on for all the even elements in the receive mode.

In a similar manner, it is possible to calibrate the odd elements in the receive mode using the even ones.

### 2.3 Extension of the calibration procedure to a 2D array

The extension of the method to a 2D array is done by using the same principles presented for the linear array, such that, calibration starts with the first elements in a row and then continues with the rest of the elements along this row. This principle can be extended to other rows, columns and diagonals according to the radiation pattern symmetries of the elements and the lattice type of the array. Two examples of possible calibration routes in 2D arrays with rectangular and triangular lattices are presented in Fig. 4. The possible calibration routes for a typical element 15 are marked in each array type.

## 3 Parametric study of the error in the calibration because of faulty elements

In this study, a linear array with  $\lambda/2$  long parallel dipoles in front of a conductive plane at a distance  $\lambda/4$  was considered. The assumptions made for calibration using MCM were: equispaced elements and array elements with symmetrical patterns. As a test case, to determine the calibration error because of violation of the equispaced assumption, one element of the array was displaced on its axis as shown in Fig. 5 and the resulting calibration error was considered. The change in distance between two adjacent elements affects the mutual coupling and inflicts a calibration error.

The mutual coupling,  $S_{1,2}$  between two  $\lambda/2$  dipoles in front of a conductive plane at a distance  $\lambda/4$  was calculated using the Kraus and Marhefka [5] closed form formula and the results are presented in Fig. 6. In the test case, a linear array of 80 dipoles was simulated. The array parameters are: element spacing,  $d = 1/2\lambda$ ; dipole length,  $l = 1/2\lambda$ , with Taylor weighting [6] (side lobe of  $-35$  dB and  $\bar{n} = 5$ ) and Bayliss weighting [7] (side lobe of  $-30$  dB and  $\bar{n} = 6$ ).

For the simulation study, element 31 was displaced  $0.013\lambda$  (3 mm for  $\lambda = 0.2308[m]$ ) to the left. The calibration process starts with the assumption that elements 1 and 2

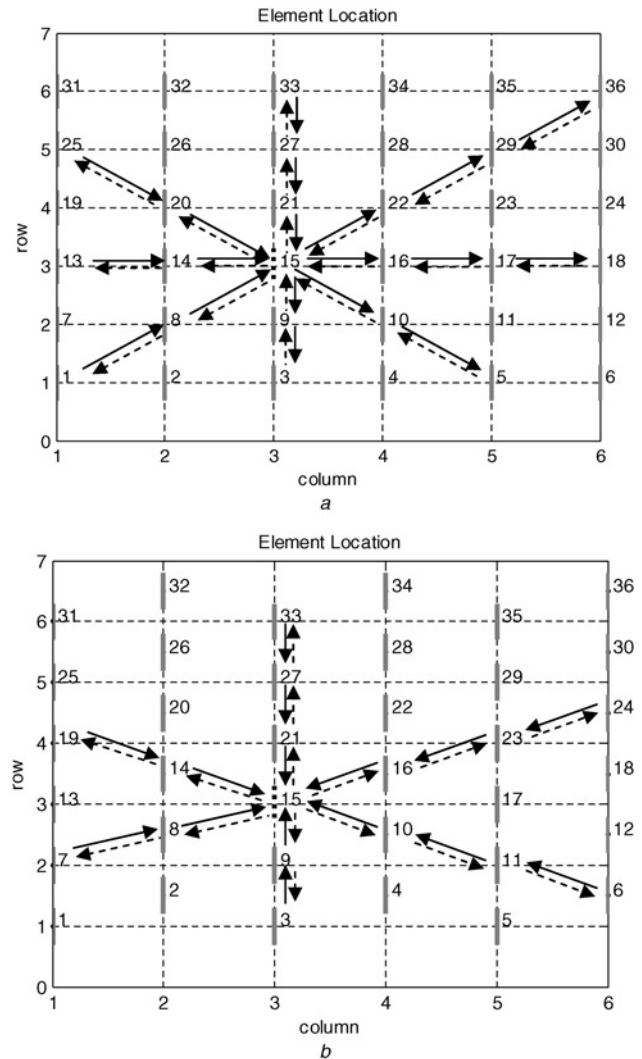


**Figure 4** Possible calibration routes in 2D arrays with rectangular and triangular lattices

a Rectangular lattice  
b Triangular lattice

are calibrated (using external instrumentation) and continues to the right (element numbers increase). The calibration results (amplitude and phase) are presented in Fig. 7. One can observe that until the faulty element (number 31) is reached there is no calibration error, whereas for the elements that follow, a calibration error is introduced and a difference between the even and odd elements is noticed. A similar calibration error result is obtained if the process starts from right to left (element number decrease), given elements 80 and 79 are calibrated. As will be revealed later, the real problem with the

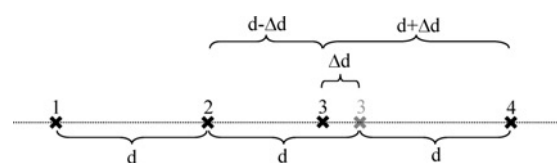


**Figure 5** Linear array geometry with one element displaced

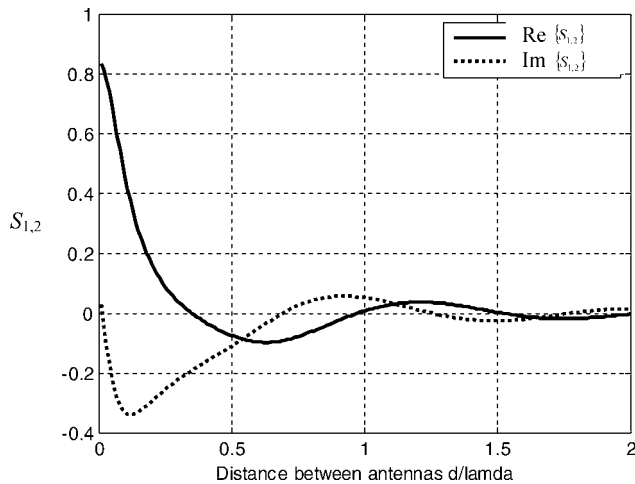


**Figure 6**  $S_{1,2}$  for two  $\lambda/2$  long parallel dipoles in front of a conductive plane

displaced element is that the error it introduces in the system not only is limited to the faulty element, but also propagates to all the elements that follow it.

In the next scenario, two faulty displaced elements (31 and 55) were considered. Both elements were moved to the left from their original positions  $0.013\lambda$  (3 mm) and  $0.0091\lambda$  (2.1 mm), respectively. The calibration results, amplitude and phase are presented in Fig. 8. One can observe that the

calibration error increases after the second faulty element (number 55). Next, the effect of the calibration error because of an element displacement (element 31 moved  $0.013\lambda$  to the left of its original location) on the array sum and difference radiation patterns (Taylor and Bayliss) was studied. The effect on the sum and difference patterns is shown in Fig. 9. In general, the effect on the radiation pattern is an increase in the far-out side lobe level. The individual calibration error effect of the amplitude, phase and combined phase and amplitude has been considered. It can be noticed that the phase error has a more dominant effect on the radiation pattern compared with the amplitude error.

Figs. 10–12 show the calibration error effect because of an element displacement (element 31 moved  $0.013\lambda$  to the left from its original location) on the sum radiation patterns for a scanning array in directions  $0^\circ$ ,  $-30^\circ$  and  $-60^\circ$  off broadside. The results for the difference patterns are similar. From the results, it can be noticed that the maximum side lobe level moves with the main beam, in the same direction while keeping about  $70^\circ$  distance between them.

Next, the effect of the faulty element location was considered. Fig. 13 shows the effect of the calibration error on the sum radiation pattern because of a displacement of elements 11, 21, 31, 41, 51, 61 and 71. From the results, one can observe the dependence of the increase in the side lobe level on the

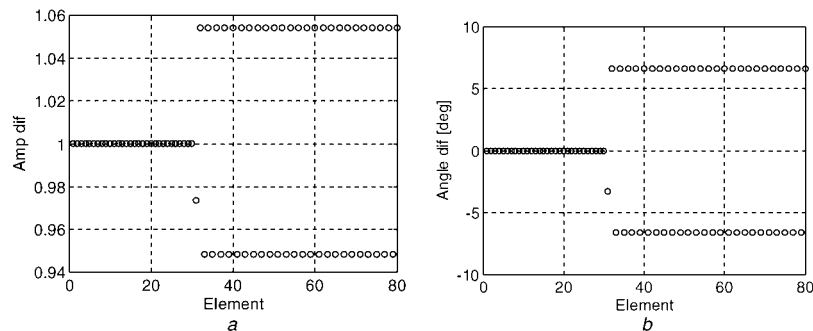


**Figure 7** Calibration results (amplitude and phase) with element 31 moved  $0.013\lambda$  to the left

a Amplitude  
b Phase

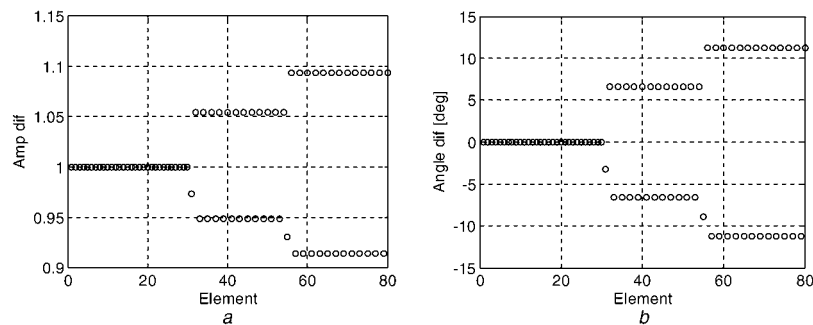


**Figure 8** Calibration results (amplitude and phase) with elements 31 and 55 moved to the left  $0.013\lambda$  and  $0.0091\lambda$ , respectively

a Amplitude  
b Phase



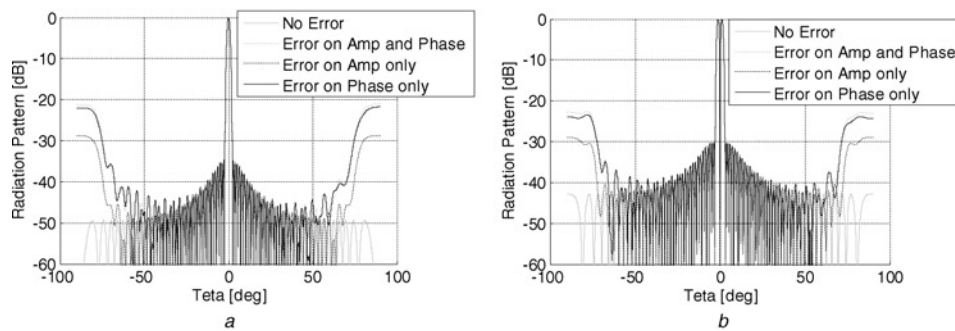


**Figure 9** Amplitude and phase error effect

a Sum patterns  
b Difference patterns

faulty element location. As the faulty element location is closer to the left side of the array, where the calibration starts, the calibration error propagates to more elements and its effect on the radiation pattern is more significant.

Fig. 14 shows the effect of the calibration error on the sum radiation pattern in the case of two faulty elements (first

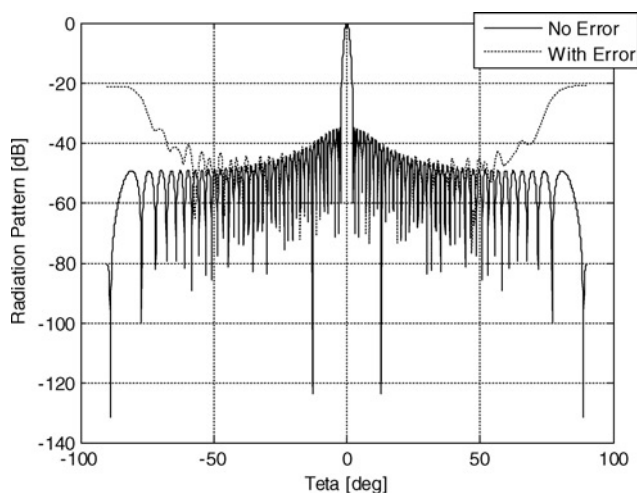


**Figure 10** Sum pattern for  $0^\circ$  scan

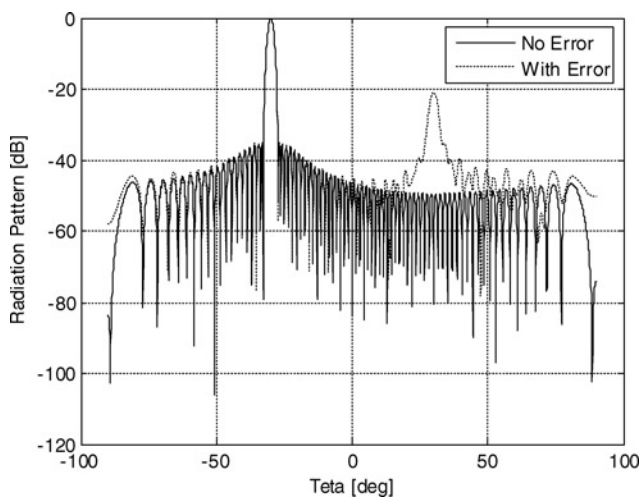


**Figure 11** Sum pattern for  $-30^\circ$  scan

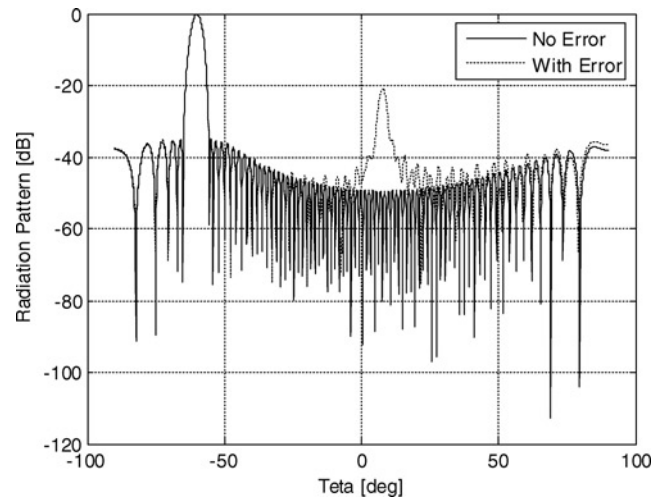


**Figure 12** Sum pattern for  $-60^\circ$  scan

displaced  $0.013\lambda$  and the second  $0.0091\lambda$ ). The first faulty element is 21 and the second is one of the elements 11, 31, 41, 51, 61 and 71. One can observe that the closer the faulty elements are to the calibration initial point, the calibration error propagates to more elements in the array and the effect on the radiation pattern is more significant, that is, an increase in the side lobe level.

## 4 Detection and bypass of faulty elements

### 4.1 Detection of faulty elements

The basic assumption of calibration with MCM is the equal coupling between adjacent elements in the array. After calibration, this assumption can be verified by examining the mutual coupling between adjacent elements over the entire array. We transmit with the even element ( $n_e$ ) and receive with the adjacent odd element ( $n_o$ ), repeat the procedure with elements ( $n_o$ ) and ( $n_e-1$ ) and so on. It is important to keep the transmitting signal (amplitude and phase) constant throughout the entire test.

If there is no faulty element, the received signal should be equal for all elements. If there is a faulty element, the received

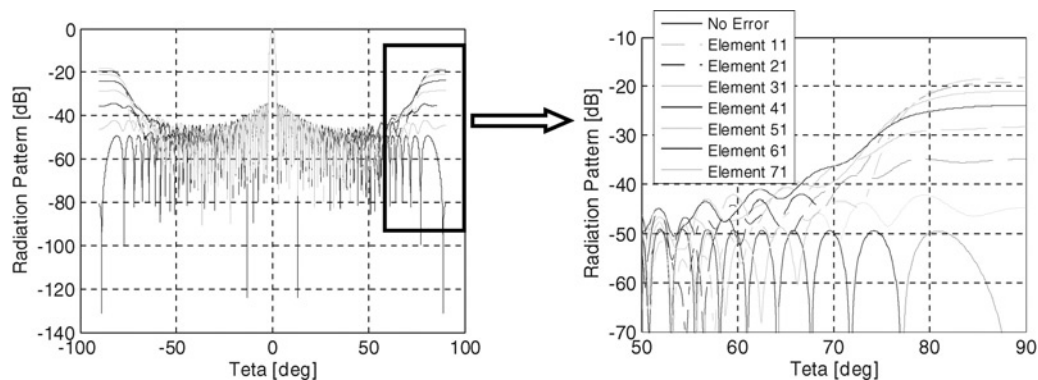


Figure 13 Side lobe levels for sum pattern with different faulty element locations

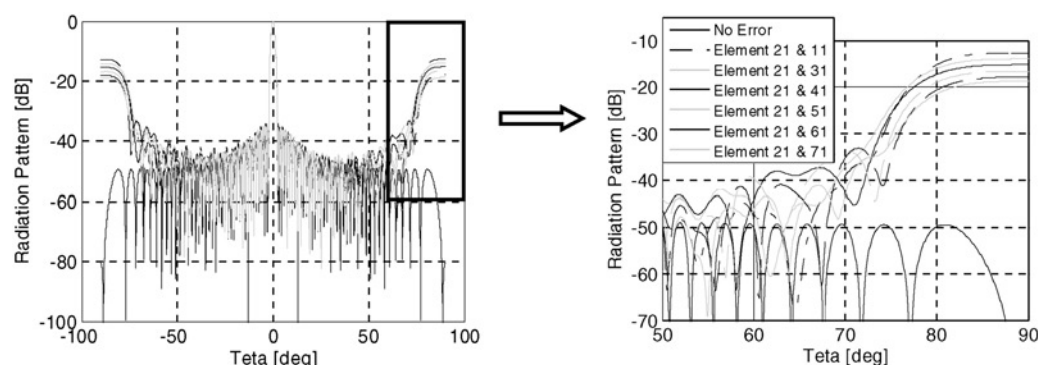


Figure 14 Side lobe levels for sum pattern with two faulty elements, one fixed (#21) and the second at different locations

signal would be different at this element and all the elements that follow it. To demonstrate the procedure, we examined the signals received by the array elements for a typical scenario with element 31 displaced to the left  $0.013\lambda$ . The amplitude and phase of the signals received by the array elements is presented in Fig. 15. One can observe a change in amplitude and phase of the signals received at element number 31 and those that follow. This is an indication of a problem with element 31, since the array is already calibrated.

### 4.2 Bypassing faulty elements

Once the faulty elements are detected, a method for bypassing them is presented. The method enables us to

bypass the faulty elements without allowing the calibration error to propagate to other elements in the array. Thus, after the calibration, only the faulty elements would remain uncalibrated and in a large array a small number of uncalibrated elements would be insignificant.

In a linear array, the way to bypass a faulty element after its detection is to resume the calibration from the opposite side until the faulty element is reached. In this way, the elements before and after the faulty element are calibrated. This method works well when there is only one faulty element. If there are more than one faulty element, the elements between the faulty ones are not reachable and cannot be calibrated.

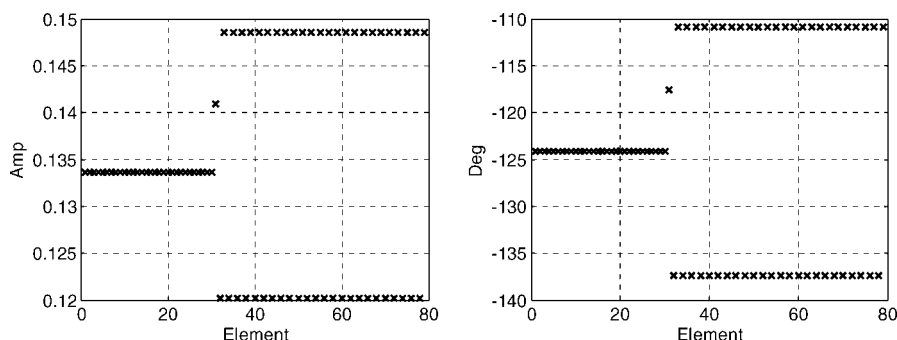
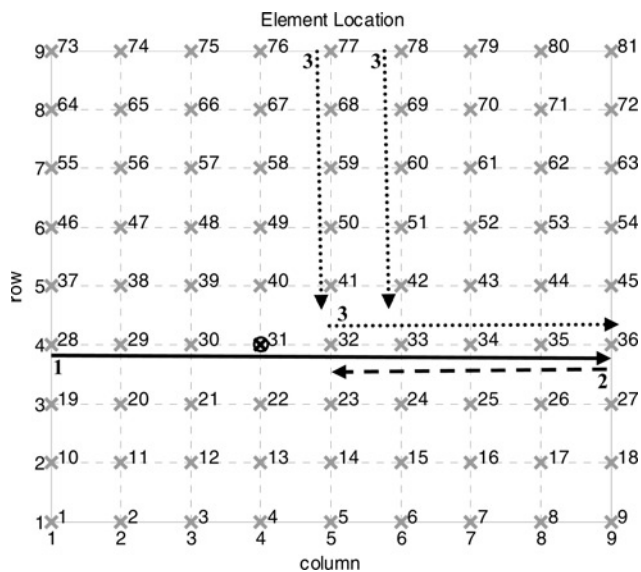
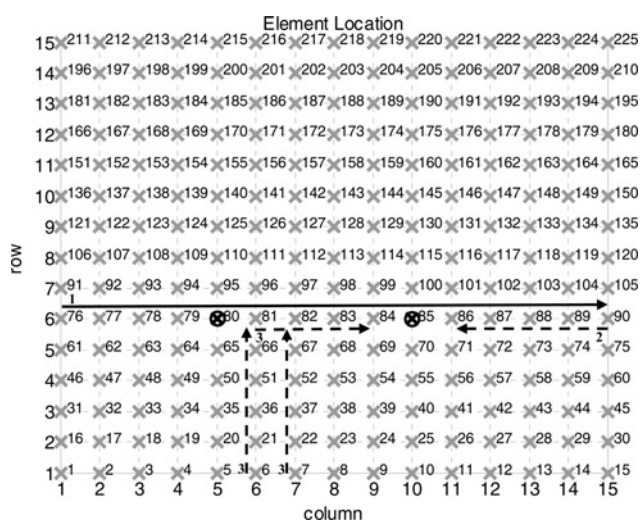


Figure 15 Amplitude and phase of the signals received by the array elements with element 31 displaced  $0.013\lambda$

a Amplitude  
b Phase



**Figure 16** Calibration routes in a 2D array with one faulty element



**Figure 17** Calibration routes in a 2D array with two faulty elements

The extension of the calibration and detection methods to 2D arrays can be done by using alternate calibration routes as shown in Fig. 4. Bypassing faulty elements in a 2D array is less complicated than in a linear array because of the increase in the possible calibration routes and the ability to reach any element from a number of different directions. Two examples of bypassing faulty elements in a 2D array are presented. In the first example, element 31 is faulty in a  $9 \times 9$  array as shown in Fig. 16. Route 1 designates the initial MCM calibration path. Routes 2 and 3 designate possible routes to bypass the faulty element 31 (after its detection) from different directions without propagating a calibration error to other elements.

In the second example, a  $15 \times 15$  array with two faulty elements, 80 and 85, is considered as shown in Fig. 17. Route 1 designates the initial calibration path through the faulty 80 and 85 elements. Once the faulty elements are detected, route 2 designates the calibration route for elements 86–90. The two routes labelled 3 are designated for calibration of elements 81–84 using elements 81 and 82 for initialisation.

The method can be generalised to consider a larger amount of faulty elements by extending the simple calibration route geometries to more complex ones, which enable to bypass the faulty elements.

## 5 Conclusions

This paper has shown that the MCM calibration technique is very sensitive to faulty elements because of the error propagation effect to the following elements. This calibration error affects the phased array radiation patterns and degrades its side lobe topology. The effect was demonstrated on the sum and difference patterns in different scenarios. A method for detecting and bypassing faulty elements was presented. The method uses the same principles of the MCM and therefore is very suitable for industrial use.

## 6 References

- [1] BERICAL H.C., CARNAHAN A.H., KRUEGER B.A., MILLER J.W., REALE D.P.: 'Self monitoring/calibrating phased array radar and an interchangeable, adjustable transmit/receive sub-assembly'. US patent 5412414, May 1995
- [2] AGRAWAL A., JABLON A.: 'A calibration technique for active phased array antennas'. IEEE Int. Symp. Phased Array Systems and Technology, June 2003, pp. 223–228
- [3] AUMANN H.M., FENN A.J., WILLWERTH F.G.: 'Phased array antenna calibration and pattern prediction using mutual coupling measurements', *IEEE Trans.*, 1989, **AP-37**, pp. 844–850
- [4] SHIPLEY C., WOODS D.: 'Mutual coupling-based calibration of phased array antennas'. Proc. Int. Con. Phased Array Systems and Technology, CA, USA, May 2000, pp. 529–532
- [5] KRAUS J.D., MARHEFKA R.J.: 'Antennas for all applications' (McGraw-Hill, 2002, 3rd edn.)
- [6] TAYLOR T.T.: 'Design of line source antennas for narrow beamwidth and low side lobes', *IRE Trans.*, 1955, **AP-7**, pp. 16–28
- [7] BAYLISS E.T.: 'Design of monopulse antenna difference patterns with low side lobes', *Bell Syst. Tech. J.*, 1968, **47**, pp. 623–640